

Running title

A practical guide to starting SEM array tomography

Title

A practical guide to starting SEM array tomography – an accessible volume EM technique

Authors

Ian J. White and Jemima J. Burden

Affiliations

LMCB, University College London, London, WC1E 6BT, UK

Keywords

Array tomography; serial section; section alignment; SEM-AT; scanning electron microscopy; volume electron microscopy; non-destructive; ultramicrotomy.

Wordcount

(11,000)

Abstract (210 words)

The techniques collectively known as volume electron microscopy (vEM) each come with their own advantages and challenges, making them more or less suitable for any specific project. SEM Array Tomography (SEM-AT) is certainly no different in this respect. Requiring microtomy skills, and involving more data alignment post imaging, SEM-AT presents challenges to its users, nevertheless, as perhaps the most flexible, cost effective and potentially accessible vEM approach to regular EM facilities, it benefits those same users with multiple advantages due to its inherently non-destructive nature. The general principles and advantages / disadvantages of SEM-AT are described here, together with a step-by-step guide to the workflow, from block trimming, sectioning and collection on coverslips, to alignment of the high-resolution 3D dataset. With a suitable SEM/backscatter electron detector setup, and equipment readily found in an electron microscopy lab, it should be possible to

begin to acquire 3D ultrastructural data. With the addition of appropriate SEM-AT imaging software, this process can be significantly enhanced to automatically image hundreds, potentially thousands, of sections. Hardware and software advances and future improvements will only make this easier, to the extent that SEM-AT could become a routine vEM technique throughout the world, rather than the privilege of a small number of experts in limited specialist facilities.

Introduction

The biology of life in all its intricate glory, exists in a vastly complicated set of interactions that, frustratingly for electron microscopists, take place in 3D. Whilst huge amounts of information has been gleaned over the years from 2D analysis, only relatively recently have significant strides been taken to allow a more routine study of the third dimension of these ultrastructural relationships, that is to perform volume Electron Microscopy (vEM). Volume EM refers to a group of recently developed imaging approaches that use scanning and transmission electron microscopy (SEM and TEM) to allow the interrogation of cell and tissue ultrastructure, at μm to mm volume scales and nm resolutions (Peddie et al., 2022). All the vEM approaches rely on the basic principle of collecting a sequential series of 2D images and reconstructing them into a 3D volume stack.

The earliest and simplest method of gaining a series of 2D EM images for 3D reconstruction is via the manual collection and imaging by TEM of a sequential series of mechanically cut and physically collected ultrathin sections in a technique known as serial section TEM (ssTEM) (Bang & Bang, 1957; Birch-Andersen, 1955; White et al., 1986). This method is accessible to those who do not have specialised vEM technology, but requires experienced microtomists and microscopists, being fraught with risk of failure at many of its multiple steps. In short, the technique requires the production of a suitable number of sequential sections in a “ribbon”. These ribbons must then be split into suitable lengths, and crucially kept in the correct order for collection onto (at largest) a 2x1mm, film coated, TEM slot grid. These grids must then be inserted into the TEM, and the region of interest (ROI) found and imaged in order in all sections before proceeding to the next grid, and so on. There is significant risk of catastrophic failure at all of these steps including, but not limited to: section ribbons failing to form and

therefore the sections not being in order; loss or damage to delicate sections at every ribbon split; loss of sections or sections ending up on non-imageable parts of the collection grid at each pick up stage; and damage to the delicate support film at any point between collection and imaging. Added to this fragility of process, the time to manually image every section, makes ssTEM an incredibly technically demanding, time and labour-intensive pursuit, and helps explain why as a technique it has generally been limited to smaller series and volumes. Longer series have been collected and imaged by particularly dedicated and experienced researchers, but generally with a very small blockface (30x150um for example) and still in the lower hundreds range (Cattin et al., 2015; Harris et al., 2006). This in part explains why much of the work on developing vEM sought to avoid the tricky sectioning and collection part of the process altogether, as well as automating the imaging. As backscatter electron SEM imaging improved to achieve closer to TEM ultrastructural resolution in biological samples, it created the possibility of developing SEM techniques to solve this problem. Focused Ion Beam (FIB, Pang et al MCB: Volume Electron Microscopy Volume 179) and Serial Blockface (SBF, Genoud et al MCB: Volume Electron Microscopy Volume 179) SEM both achieve this by imaging the blockface of the sample itself. Whilst solving many of the problems associated with ssTEM as described above, they introduce a new set of difficulties and limitations, such as being destructive one shot techniques precluding the ability to reimage samples, requiring alternative sample preps and resin embedding protocols, struggling to image bare resin areas without charging issues, and necessitating additional equipment such as an automated microtome to be added to the SEM chamber or having an expensive FIB in the SEM. Blockface techniques also require the user to start their imaging "blind", estimating where their ROI will appear in the block before it is eventually revealed by the cutting process, and where in X and Y it may subsequently go as imaging proceeds through the depth of the sample. SEM Array Tomography (SEM-AT) exists almost as a hybrid of these two approaches; a technique that avoids the new disadvantages of the blockface SEM techniques, and preserves the advantages of ssTEM whilst mitigating the difficulties described. Whilst certainly not without its problems and limitations, SEM-AT's hybrid approach allows it to occupy a niche which makes it the optimal protocol for certain samples.

Rationale

SEM-AT was a term first formalised in 2007 (Micheva & Smith, 2007). Simply put, array means an ordered series or arrangement, and tomography derives from the ancient Greek to write, or describe (image in this case) a slice. Put another way, SEM-AT could perhaps more helpfully be described as serial section SEM, as such it is very easy to see it essentially as a user-friendly upgrade to the ssTEM as described above. Many of the pitfalls of ssTEM are due to the limitations introduced by the use of the TEM itself and are avoided or mitigated by use of an SEM, others to the process of ribbon splitting and collection onto delicate grids which are also ameliorated by use of a larger and more robust collection substrate.

The basic steps of the SEM-AT workflow, summarised in Figure 1, can be broadly split into two phases. 'Section Preparation' including sample preparation and embedding (Fig. 1A), sectioning (Fig. 1B), section collection (Fig. 1C) and mounting (Fig. 1D); and 'Section Imaging' including automated SEM imaging (overview, Fig. 1E; section outlining, Fig. 1F; ROI acquisition, Fig. 1G) and post-acquisition processing, (Fig. 1H).

[insert Figure 1 here, full page width]

Section Preparation: ssTEM vs SEM Array Tomography

ssTEM and SEM-AT are similar in the first 'Section Preparation' stage, but the finer detail differs as shown in Figure 2. Samples for either technique must be fixed to retain their ultrastructure accurately, heavy metal stained, dehydrated and embedded in resin (Fig. 2A). A blockface must be trimmed and a ribbon series of sequential sections cut on a microtome. The ribbon must be split into suitable size lengths and collected on a support substrate, upon which they can potentially be further section stained before imaging in the appropriate microscope. What differs is that the constraints of section thickness required to pass an electron beam through for TEM is removed allowing thicker section collection, and the size constraints of the fragile 2mm x 1mm film coated TEM slot grid (Fig. 2a-d) is replaced by the use of significantly larger and more robust silicon wafer, glass coverslip/slide (Fig. 2i-iv) or section tape. The larger collection substrate allows for the cutting of large area blockfaces incorporating more material for

imaging in each section, whilst still allowing many hundreds of sections to be collected at once. The larger and less delicate collection substrate also means far fewer ribbon splits, section collection steps, and reduced risk of sample damage post collection than previously described for ssTEM. Immediately, SEM-AT becomes more accessible to less experienced microtomists and more robust than ssTEM.

[Insert Figure 2 here]

Section Imaging: ssTEM vs SEM Array Tomography

As expected, the microscopy phase of an SEM-AT workflow differs more significantly from that of ssTEM. The ability to put much larger samples into an SEM chamber than the TEM means that all sections in a collected sample can be in the chamber and available for imaging at one time. Imaging can then take place of hundreds of sections over a large area, expanding the volume available for image acquisition vastly. With all sections available for imaging in the microscope at the same time, it is easier for software to automate acquisition throughout the whole section range collected. After setting up suitable imaging parameters and choosing an ROI, the section series can then be imaged in order, one after the other, at the required resolution. After this image series is acquired, further imaging can be performed on the same section set, either of the same ROI at a different resolution or a different ROI.

Advantages and disadvantages of SEM Array Tomography

Whilst SEM-AT holds many advantages over its vEM cousins such as ssTEM, SBF-SEM and FIB-SEM, there are also some significant disadvantages associated with the technique. Whilst hugely more manageable than ssTEM, the microtomy of blockface preparation, sectioning, ribbon splitting, and section collection still require some expertise. The Z resolution of imaging will also be defined by the thickness limit at which one can reliably collect sections. Sectioning for SEM-AT can be thicker than for TEM, as there is no requirement to pass the beam through the section, however, the lower limit of what can be cut, whilst sample dependent, is probably about 40-50nm. This compares unfavourably with SBF-SEM, where as little as 20nm

can be reliably removed from the block between imaging (Chen et al., 2017; Wanner et al., 2015), and more significantly with FIB-SEM, where 4nm of the block can be milled away (Xu et al., 2017). Another potential disadvantage is the increased risk of introducing physical distortions in the sections during the mechanical cutting process, which can yield inaccuracies and require more post image acquisition processing to align the images into a smooth 3D volume.

The advantages, however, are significant and make it a particularly apt vEM choice for certain samples. The foremost of these is the non-destructive nature of the technique. Unlike SBF-SEM and FIB-SEM where the surface of the block is removed and destroyed/discarded before the blockface is imaged, and thus that material, no matter how interesting can never be re-imaged, SEM-AT allows the repeat imaging of sections. This can mean reimaging the same ROI at a different resolution, reimaging a different ROI in the same section set, reimaging regions of new interest that have only become apparent post the first round of acquisition, or reimaging for failed acquisition e.g. poor focus. Therefore, SEM-AT could be applied to precious samples eg. clinical biopsies, that need to be retained for future reference. A second major advantage is that all of the Z information is immediately laid out prior to high resolution imaging. The ability to capture a first round of lower resolution imaging, can greatly facilitate choice of final ROI and ROI tracking for structures that drift in X and Y, and/or meander through the depth of the sample. This allows the researcher to only image the sections and the area of each section where the ROI is present, increasing efficiency and throughput by saving significant amounts of time imaging, as well as reducing the overall dataset size – aiding downstream computational demands with alignments, analysis, sharing and storage. Thirdly, the collection of these sections on a conductive substrate reduces charging effects when imaging large areas of bare resin which is sometimes inevitable e.g. cell culture monolayers towards the top of the cell compared to blockface techniques. Fourthly, as sections have been cut and the tissue exposed, SEM-AT samples are amenable to staining for on-section CLEM with all the advantages that brings, if the preparation and resin are suitable. Finally, as additional heavy metal stains can be applied to the collected sections, it creates the possibility of leveraging the wealth of legacy samples, not initially prepared with vEM in mind, which can still be explored by SEM-AT.

As such SEM-AT is a powerful, flexible, vEM technique that fills a niche for samples and imaging strategies that are not as well served by other vEM techniques.

KEY RESOURCES TABLE

Note that not all areas will be used in every protocol

REAGENT or RESOURCE	SOURCE	IDENTIFIER
Chemicals, Peptides, and Recombinant Proteins		
Chloroform	Fischer-Scientific	C/4960/PB08
Contact cement - DAP Weldwood	DAP	107
Poly-L-Lysine	Sigma	P 8920
Silver DAG	Agar Scientific	G3691
Triton X-100	Sigma	T8284
Xylene	TAAB	X001

MATERIALS AND EQUIPMENT

- Diamond knife suitable for ultrathin sectioning with large boat
- Single edge razor blades
- Trimming diamond (optional)
- Ultramicrotome with water withdrawal device
- SEM with array tomography software, sensitive backscatter electron detector, stage bias (ideal, but optional)
- SEM stubs, large enough for the ITO coverslips and compatible for the SEM stage
- Carbon stickies that are compatible with the SEM stubs
- Indium Tin Oxide (ITO) coated coverslips 22mm square, no.1.5 8-12ohms/sq
- Multi-meter to measure resistance
- Paint brush e.g. size 0 pure sable brush

- Eyelashes on cocktail sticks (three, one dedicated for use with contact cement)
- Silicon tubing to fit ultramicrotome water withdrawal device
- 10ml syringe
- Dispensing needle, short, blunt end, 14 gauge
- Paperclip large e.g. 5cm
- Pliers
- Sticky tape
- Permanent marker
- Ruler
- Forceps for handling coverslips
- Heat block suitable for 60°C.

BEFORE YOU BEGIN

Buffers/Materials to be made up in advance

- Contact cement -dilute contact cement with xylene, 1:1 (it shouldn't be stringy)
- Triton X-100- prepare a 0.1% solution with distilled water
- Poly-L-Lysine- prepare 1% and 0.1% solution with distilled water
- Silver DAG – dilute with manufacturer supplied diluent following manufacturer's instructions.
- Check and mark coverslips with a permanent marker so that ITO coated side is identifiable.

Prepare Jumbo Ultra diamond knife for array tomography sectioning

1. Take a large paperclip and roughly straighten. Using pliers, bend the paperclip to fit across the width of the Jumbo Ultra diamond knife with loops on either side (Fig. 3A) to secure over the edges of the boat and allow the middle section to rest on the base of the boat, (Fig. 3B).

Note: this paperclip once prepared can be reused.

2. Place the Jumbo Ultra diamond knife into the knife holder, taking care to set the knife cutting angle to that specified by the diamond knife manufacturer. Place a 22mm square coverslip

into the knife and roughly position the paperclip to support the coverslip in such a way that the rear edge of the coverslip is resting on the back of the diamond knife boat, and out of the boat (Fig. 3B and C).

3. Secure the paper clip with two small pieces of tape, one on each side, taking care that the tape does not reach over the top edge of the boat (Fig. 3C).
4. Fill the boat with water and adjust level of the water so that the water is slightly concave at the knife edge. Then readjust the position of the coverslip (replacing the tape if necessary) so that the paperclip ensures that the coverslip sits stably in the boat, with the rear edge just slightly out of the water (Fig. 3B and C).

Note: take note of where the water level reaches on the 22mm coverslip when the boat is filled with water to the correct level for sectioning. This indicates the line, up to which poly-L-lysine can be coated to aid section attachment at a later stage (Fig. 3D).

5. Once the paper clip is in the correct position, remove the water, clean the diamond, dry completely and store until needed.
6. To aid the collection of ribbons of the correct length, using a ruler and taking care not to touch the diamond, measure 18mm, horizontally back from the diamond, making a small mark on both sides of the knife boat (top edge) (Fig. 3E arrowhead).

[Insert Figure 3 here]

Prepare water withdrawal device on ultramicrotome

1. Connect one end of the silicone tubing to the water withdrawal device that comes with the microtome, as shown in Fig. 3F.
2. Connect the other end of the silicone tubing to a blunt dispensing needle. If necessary, wrap a little parafilm around to secure the connection.
3. Connect a 10 ml syringe that has been previously rinsed out several times with distilled water, to the dispensing needle.

Prepare ultramicrotome for serial sectioning

1. If possible, set up pre-set ultramicrotomy modes for:
 - a. Ultrathin sectioning e.g. 70nm
 - b. Ribbon splitting e.g. 5nm

A note about sample preparation

Unlike sample preparation for the blockface imaging techniques (FIB-SEM and SBF-SEM), sample preparation for array tomography is a little less restrictive. In part, this is because the absence of the large bulk of non-conductive resin reduces imaging challenges relating to charge, but also due the fact that, if necessary, additional stain can be introduced to the sample, after sectioning. Numerous good protocols and reviews cover sample preparation for vEM techniques (Deerinck et al., 2022; de Schepper et al., 2022; Peddie et al., 2022, Narayan et al MCB: Volume Electron Microscopy Volume 179), which are also suitable for SEM-AT, but equally we have successfully performed SEM-AT on samples conventionally prepared for TEM and then post-stained with lead citrate after serial sections are collected on coverslips.

STEP-BY-STEP METHOD DETAILS

Trimming and Ultrathin Sectioning

Timing: 1 hour + depending upon the number of sections required.

The region and size of the blockface, will likely be dictated by the research question, ensuring the capture of the whole ROI in X, Y and Z. The size of the blockface and number of sections required can impact the choices made regarding, size of support substrate required, the type of diamond knife and potentially the type of ultramicrotome used (see discussion for further information). To save space on the support substrate, reduce sectioning and pick up times, as well as ease of imaging in the SEM later, working with the smallest blockface that addresses the research question is recommended. The following protocol describes a workflow using a Jumbo Ultra diamond knife with a standard ultramicrotome, whilst collecting sections onto a 22mm square ITO coated coverslip. This

size coverslip can support for example, ~600 ultrathin sections, from a blockface of dimensions ~1mm x 0.5mm. This represents a volume of ~21,000,000 μm^3 ; 1000 μm x 500 μm x 42 μm (assuming 70nm slices). It is recommended to be already proficient at ultrathin sectioning prior to attempting this protocol with precious samples and to ideally serial section in an environment free of vibration and drafts.

1. Using a single edge razor blade carefully trim to a blockface that is marginally larger than your ROI in X, Y and Z.
 - a. **Critical:** leading and trailing edges must be parallel
 - b. Ideally the blockface would be:
 - i. Asymmetric (to allow immediate identification of ribbon direction and therefore Z relationship of sections)
 - ii. With the leading edge being larger than the trailing edge (to aid smooth sectioning).
 - iii. Slopes of the blockface relatively steep e.g., Between 10-30 degrees from the vertical, see Fig.4, (to prevent sections getting significantly larger as longer arrays are collected).

[Insert Figure 4 here]

2. Optional: Using an eyelash, apply a small droplet of contact cement to the slope of the leading edge, allowing the droplet to flow upwards to the leading edge of the blockface. If necessary, gently encourage this with the eyelash, as shown in video 1. Allow to dry.

Alternatives: Pattex (personal communication Helmut Gnaegi), or quality hair spray (Harris et al., 2006).
3. Place the specimen arc into the sectioning arm of the ultramicrotome.
4. Place your Jumbo knife with paper clip assembly onto the stage of the ultramicrotome, adjusting the cutting angle if necessary.

5. Take a 22mm ITO coverslip and dip 90% of the coverslip into 0.1% poly-L-lysine, leaving ~2mm uncovered, as shown in Fig. 3C, then place the coverslip, ITO side up, in the knife assembly.

Alternatives: Glow discharging coverslips is another method for altering the hydrophobicity of the substrate.

6. Position the water withdrawal device on one side of the knife, positioning the end of the water withdrawal needle to the lowest point of the boat, angling the silicone tubing away from the user, Fig 3D. Secure the silicone tubing loosely with tape to the microtome body, Fig. 3F. This keeps it out of the way when cutting and reduces the chance of transferring vibrations to the boat water when removing water with the syringe.
7. Overfill the boat with filtered, distilled water, so that the level is slightly convex, but not overflowing, Fig. 3D. Use the syringe to withdraw water to the appropriate level for sectioning, e.g. slightly concave at the knife edge, Fig. 3E. Check the water interface at the edge of the coverslip. Ideally it will be flat, at 80-90% of the length of the coverslip. If necessary, use a paintbrush to “paint” a line of 0.1% poly-L-lysine at the top edge where the water/air interface will be, on the ITO side. Once satisfied, withdraw more water from the boat, so that the diamond knife is dry for alignment.
8. Align your block and diamond knife, using specimen rotation, knife rotation and specimen tilt to ensure that the knife is equidistant from the entire blockface.
9. Add water to the boat so that the water is slightly concave at the diamond knife and flat at the contact with the ITO, poly-L-lysine coated coverslip.
10. Optional: Add a single droplet of 0.1% Triton X-100 to the water to aid section handling.
11. Start ultrathin sectioning, taking care to observe the length of the ribbon, as it is produced, with respect to the 18mm ribbon length marker on the side of the knife boat, Fig. 3E arrowhead.
12. As the end of the ribbon approaches the 18mm mark, prepare to split the ribbon using one of the following methods (as shown in video 2):
 - a. Quickly split the ribbon “on the fly” without pausing the cutting program, during the return stroke of the specimen arm.

- b. Switch the sectioning mode to “5nm ribbon splitting” thickness for 2-3 cuts then return the ultramicrotome to “ultrathin sectioning” (personal communication, Rêza Shahidi).
- c. Pause the cutting program during the return stroke and gently detach the ribbon from the diamond by dragging an eyelash over the diamond edge. Retract the sample by 200-500nm and restart the cutting program.

Caution: if using chloroform in step 17, take into account potential section expansion upon chloroform treatment, when predicting the length of your final ribbons.

- 13. An eyelash can be used to gently waft the first ribbon to the side of the boat, out of the way of the next ribbon.
- 14. Steps 12 and 13 can be repeated numerous times until several ribbons have been collected. After the sample has passed the knife edge, pause the cutting. Use eyelashes to gather and dock these first ribbons to each other, side by side, in the correct order. This reduces the chance of ribbons getting mis ordered later.

Alternative: depending upon the length of ribbons and the microscope configuration, it may be advantageous to collect ribbons in a snaked format. This causes the distance between the last section of a ribbon and the first section of the subsequent ribbon to be closer to each other when imaging in the SEM. This can impact the tolerances required for auto-functions when automated imaging and may be critical if ribbons are particularly long. **Caution:** if drafts are present, it may be necessary to dock only a couple of ribbons at a time.

- 15. Repeat steps 12-14 until enough sections have been collected for your research question or enough ribbons have been collected to fill one coverslip (whichever happens first).
- 16. Using eyelashes, dock all ribbons together side by side.
- 17. Using a glass rod, hover a drop of chloroform over the ribbons to allow the sections to stretch out, taking time to observe and aim for even treatment across the ribbons.
- 18. Ideally, all sections and ribbons are still in order and docked as one group, if not, use eyelashes to rearrange ribbons and/or rogue sections.
- 19. Using eyelashes, and adjusting the position of the oculars as necessary, gently move the ribbons towards the ITO coverslip:water surface interface. Gently, dock the leading edge of the ribbon collective to the coverslip surface. Ideally, the ribbons will be collected in such a

way that the leading edge of each ribbon can be docked to the coverslip. However, if not, then docking just some of the ribbon ends to the coverslip, should be sufficient as all ribbons are still attached to their adjacent neighbours, which should prevent any escaping upon water withdrawal.

20. With an eyelash in one hand and the water withdrawal syringe in the other hand, slowly, evenly, and gently remove the water from the boat, whilst ensuring that the ribbon collective remains attached to the coverslip, as shown in video 3.

Caution: use the eyelash to round up any stray ribbons or sections.

21. Once the water is drained from the coverslip, and the sections are settled on the coverslip surface, use forceps to transfer the coverslip to the 60°C heat block, section side up, to dry.
22. Ensure that the coverslip is completely dry before proceeding to mounting.

Sample mounting

Timing: 10 minutes + drying time

23. Label the underneath of an appropriately sized SEM stub, then firmly stick a double-sided carbon sticky to the top of the SEM stub and remove the upper protective backing.
24. Carefully mount the ITO coverslip (serial sections facing upwards), to the centre of the stub, taking care not to touch/damage the sections.
25. Using forceps, gently press down on the coverslip on section-free areas to ensure good contact with the carbon adhesive.
26. Using a cocktail stick or a similar tool, apply silver DAG to the edges of the coverslip that have space to contact the carbon sticky, taking care to ensure silver contact reaches; the top of the coverslip (not too near sections), the carbon sticky and the SEM stub itself (Fig. 1D).
27. Allow the sample to dry in a dust free environment, e.g. fume hood.

Imaging for Array Tomography

Timing: hours to days depending upon ROI size in X, Y and Z and SEM and detectors used.

The non-destructive nature of SEM-AT informs the basic imaging strategy. Samples are repeatedly scanned in increasing levels of resolution, usually in decreasing areas, as the ROI is defined and imaged. This process requires several key functions to be realistically achievable. Firstly,

a fast and sensitive backscatter detector to image sections rapidly at low kV to prevent sample damage. Focus, stigmation and stage movement must be automated and accurate, mosaic stitching must be possible to provide coherent pictures of large areas, tools to define individual sections and further define ROI for imaging must exist, and preferably this all has to be brought together in one user friendly software package.

The following protocol describes the general principles and workflow of SEM-AT imaging irrespective of imaging equipment specification/manufacturer used. However, some details given are specific to our system which is: Zeiss Gemini 300 FEG SEM-AT high vacuum with SENSE backscatter electron detector and Tandem Decel stage bias system, using ATLAS 5 software for automated array tomography image acquisition.

Optimising imaging conditions

Firstly, set up basic parameters to achieve high quality images on an unimportant part of a sample before further imaging. This will be sample and microscope dependent, however, the following are factors to consider:

- Set the sample to a working distance optimized for the backscatter detector as advised by microscope manufacturer.
- Adjust beam voltage to obtain a satisfactory image without inducing beam related damage/artefacts.
- Adjust pixel dwell/imaging time to achieve an optimum signal to noise ratio without inducing charging effects/sample movement/darkening.
- Adjust brightness and contrast to suit.

Optimizing imaging parameters can be a protracted but worthwhile process, and an optimised protocol for one sample can be a good starting point for optimisation on a similar sample. In our system we begin with an accelerating voltage of 4.5kV reduced to a landing energy of 1.5kV via a 3kV stage bias, and tailor the pixel dwell time according to resolution required for the particular type of imaging (0.2-2 μ s per pixel).

Once optimised, the rest of the process is performed in specific array tomography software, be it ATLAS 5 in Zeiss, Maps in Thermo Fisher Scientific, SEM Supporter/SEMography in Jeol or ACAT in Hitachi systems, for example.

Mapping ribbons

The initial image acquisition stage requires mapping of the ribbons in their entirety into the array tomography software. This is achieved by drawing a bounding box around the section ribbons and utilizing a high speed low resolution imaging protocol e.g. 600nm pixel size and sub microsecond pixel dwell time without auto functions, (video 4). Ribbon outlines for bounding box positioning are ascertained either by live image, alignment of multiple SEM visualised points with an existing optical camera image, or by SEM still images of outer ribbon extremities. The final aim is to visualise with sufficient resolution to show individual section boundaries, and roughly see the cells/tissue structure in each section.

Section delineation

For the software to move between sections accurately and automatically, it has to be informed where each section is, and in what order they should be imaged. This exact process differs slightly for different softwares but follows similar principles and is usually semi-automated.

An area is marked on the first section and placed specifically with regards to section X and Y stage coordinates and orientation. In Hitachi and Jeol systems this is a simple line along one edge of the section, in Zeiss, and Thermo Fisher Scientific systems, an outline of the section, Fig. 5A-B. Once the section marker is placed on the first section, the marking of the rest of the array sections is completed in various semi-automated fashions. Thermo Fisher Scientific software for example will auto detect all sections, but requires user input to define section order, and manual addition/adjustment to account for software error. Zeiss snap section tool uses the section outline to automatically “snap” the section marker to each new section with a mouse click (video 5). Should the automated section recognition systems struggle however, manual placement and adjustment for each section is still possible.

Section boundaries can sometimes prove a difficult way to define sections throughout a long section series. Due to the varying angle of the sloping sides of the block the section size and geometry can change significantly over hundreds of sections thus making it difficult to accurately (within nanometers to micron) place this section marker over every section (see Fig.5A-C). Alternatively, a problematic sectioning run can result in poor ribbons of sections with overlaps,

damaged edges and therefore modified section outlines. In these circumstances an alternative method involves defining a rectangle, aligning the long edge parallel with the section leading or trailing edge to achieve correct rotation, and then placing the centre of this rectangle on a feature constant throughout the array, (Fig. 5C), which requires sufficient resolution. After initial ribbon mapping, it may be necessary to map the sections at a higher resolution, for example 200nm pixel size, to visualise an appropriate feature, this is also beneficial to accurate section placement by the automated systems and is often necessary for identification of sample features for later selection of ROI. Whilst accurate manual section marker placement and/or fine adjustment of automated placement costs time, the accuracy of final section marker placement is crucial for accurate automated placement of all future ROI markers.

[Insert Figure 5 here]

Note: If an on-section CLEM experiment is being performed then the sections will already have been defined in the LM imaging stage, and sometimes this data and imagery can be imported meaning this step can be bypassed.

ROI selection and placement

The software now has a map of all the sections, their order, stage coordinates and orientation. This allows the software to calculate the position of any ROI in all sections, given its position and orientation in any one of them. The user selects their ROI in any section that includes the feature they wish to image by drawing around that feature with an ROI selection tool. The ROI is then automatically propagated to all other sections in the array, with some systems using feature recognition/tracking between images to account for stage imprecision, inaccuracies of section marker placement, section shape variation etc which might potentially result in the ROI being placed incorrectly. Even with automated assistance, there will always be small inaccuracies, part of your feature may drift in X and Y or the feature as a whole expand through the section set, so using a bigger ROI size than strictly necessary ensures that the feature of interest is still captured in each image. This also enables cropping post image series alignment without distracting image borders appearing.

Usually, ROI markers of different geometries are available. It is worth considering at this point the advantage of limiting the number of pixels in your final image and thus reducing imaging time, against the aesthetics of your final image stack, (Fig. 5D-F). A circle with a diameter equal to the length/width of a square covers 78.5% of the square's area, and consequently only takes 78.5% of the time to image, so maybe a sensible choice, Fig 5D. An intricate polygon around an ROI on the other hand may save time at the imaging stage, but post acquisition and alignment it may not be the best for presentation purposes.

Following the automated propagation of the ROI marker it is both possible, and prudent, to check that it has placed correctly throughout all sections. This process can also be used to note which range of sections the feature actually appears in, rather than imaging the whole array of sections if this is not necessary. In our experience, no matter how accurately one has attempted to place the section markers, the ROI placement after automated propagation is usually not 100% accurate and needs minor manual adjustment in some sections. Once the ROI placement has been checked and the section range in which the feature of interest appears noted, then high resolution imaging can begin.

ROI Imaging

Optimising imaging parameters before embarking on a full-scale acquisition of your ROI throughout hundreds of sections, is time well spent. Considerations include resolution required in terms of pixel size, dwell time, tile size, whether mosaic stitching will be required and auto-function settings.

Resolution is crucial to final image quality, the trade-off being that a twofold improvement in resolution by halving the pixel size, results in an image containing four times as many pixels; quadrupling the acquisition time and data. Therefore, a balance is to be found imaging at or just beyond the required image quality required rather than always imaging at the highest possible resolution. Should this resolution in hindsight not prove sufficient, reimaging of the sections at a higher resolution (maybe in a smaller ROI) may be performed at a later time, due to the non-destructive nature of the process.

For efficient imaging, appropriate pixel dwell time should be ascertained with a series of test images. Small changes in pixel dwell time can have huge impact on acquisition time over large fields

of view comprised of millions of pixels, and image series over hundreds of sections, so the minimal time without compromising on image quality should be selected, with perhaps a small margin to account for imaging differences between sections.

Any image requiring mosaic tiling will have an impact on acquisition time as overlapping areas have to be imaged, and software stitching of tiles must take place. If possible, it is wise to avoid/minimize the need for tiling. This can be achieved through a variety and/or combination of mechanisms, e.g. altering ROI shape and/or size, where the current size or shape goes just over the threshold requiring extra tiles; or by a small change in pixel size, where this allows the field of view required to fit inside fewer tiles.

Autofocus and auto stigmation settings are usually determined by the user in terms of frequency, location and parameters. This is another stage where it is worth spending time testing and optimizing. The aim is to specify auto functions that are quick, reliable and flexible enough to work on a range of contextual features in the sample and across the distances between sections, including those at the end of one ribbon and start of the next. Auto functions may also be specified to be performed on a suitable (i.e. not bare resin) area that is separate but adjacent to your ROI to avoid the risk of leaving imaging marks on your final data. Adjustable auto function parameters usually include pixel dwell time, pixel ratio, frequency of operation: whether performed on every tile, every mosaic of tiles or every nth tile/mosaic, and in some cases focus range.

Once this process of optimisation and parameter setting has taken place, it is simply a matter of selecting the range of sections you wish to image the ROI in. Omitting sections where the ROI is obscured by dirt/section folds etc, may be prudent, as this can interfere with auto functions and subsequent imaging. Imaging should then occur automatically and sequentially without further input until the desired series has been completely acquired.

Re-Imaging/Further imaging

Following series acquisition the data should be assessed. Any sections where imaging is unsatisfactory due to misplacement of ROI or failed auto functions resulting in a low-quality image, for example can be reimaged until satisfactory results are achieved. Further ROI can be placed and acquired following the process described above, though less optimisation should be required. New ROI can be in the same area at a different resolution or completely new areas as required.

Image alignment

Timing: 10mins to hours, depending upon the data size and computational resources

Alignment of images of physical serial sections is usually more challenging than aligning images from blockface techniques. These challenges are introduced in part because the sections are physically collected. Collecting sections, can introduce physical distortions and damage/debris can be incorporated during handling, collection and storage. Additional rotational and translation alignments are required because ROI that are placed and imaged in each section are rarely completely accurate across the ribbons, so some trimming of the dataset after alignment will likely be required.

Alignment can be an iterative process and depending upon the ultimate research question and type of analysis planned, various alignment strategies may be used. An initial alignment will be required to visualize the biological sample as continuous ultrastructural features. This can be beneficial before exporting the data from the SEM, as it allows the researcher to accurately specify the regions of the data for export in X, Y and Z and reduces the need to work with unnecessarily large and unwieldy datasets. This level of alignment may be sufficient for analysis where qualitative analysis or quantification of the number of events (contacts, cell types) is required. If 3D segmentation is required, then additional alignment steps are likely to be needed.

There are numerous software packages, plugins, scripts and solutions, both commercial and open source, that include some aspects of serial image alignment or registration, many written specifically with serial EM images in mind. These include, Fiji/Image J (Schindelin et al., 2012) – TrakEM2 (Cardona et al., 2012), Register Virtual Slices, Linear stack alignment using SIFT (Lowe, 2004), IMOD (Stalder et al., 2013), Amira (Stalling et al., 2005). These softwares can vary in terms of file formats required and the way the applications utilise the computational resources available.

Irrespective of the software used, an initial rigid transformation alignment, making rotation and XY translational changes between sections is a sensible and common starting point. Affine alignments, which include flexibility for alterations in shear and shrinkage between images, is also possible. Whilst these physical distortions can occur during the sectioning and pick up process, and are potentially present in the sections, in our hands, these algorithms are often less reliable, producing what appear to be beautifully aligned stacks on some datasets and wildly inaccurate alignments in others. As most alignment algorithms are based on cross-correlation or scale invariant

feature transform (SIFT) methods, using texture and features in the images as references, caution should be taken when aligning data with features that collectively track across the dataset in X or Y, or collectively spiral. This is to avoid artificially straightening the data. If possible, including features that migrate through the Z stack in multiple directions, will minimize this risk. Regardless of what alignment strategies are used, resulting aligned stacks should be “sense checked” by carefully observing the stack, scrolling first through the XY planes, and then XZ and YZ planes. Ultimately, any small inaccuracies or mis-alignments can often be manually corrected, prior to cropping the dataset and 3D reconstruction/analysis.

Discussion and advances

Array tomography is a non-destructive EM approach that provides 3D ultrastructural information of cells and organelles at nm resolutions across micron scales. Whilst it is an extremely flexible approach, permitting the imaging of samples that require post section staining, or reimaging of samples for different resolutions, ROI etc, it has its limitations. The only insurmountable limitation is Z resolution, a feature constrained by the thickness of the physical sections able to be collected. For many research questions, this reduced Z resolution will be irrelevant. However, some research questions will require finer Z resolution, therefore SBF-SEM or FIB-SEM should be considered as potentially more suitable vEM approaches. The remaining limitations relating to the challenges associated with collecting and automated imaging of serial sections and alignment of resulting images, are however constantly being ameliorated by significant advances in the fields of ultramicrotomy, SEM hardware and software design, as well as computational advances.

Ultramicrotomy advances:

Ultramicrotomy has been an essential skill for electron microscopists since the dawn of TEM, however, collecting many serial sections, in order, without loss on TEM grids was then and still is, exceptionally challenging. Over time, skilled microtomists have developed techniques to aid this process, including those described here e.g. blockface asymmetry and pickup methods to know order of serial sections, the use of adhesives to aid serial section cohesion and the stability of ribbons etc, but the advent of automated array tomography using the SEM has resulted in a surge of additional developments.

Diamond trimming knives are commercially available, creating blockface slopes of specified angles. These remove the need for steady-handed, manual trimming with razor blades and control the proportional increase in size of serial sections as they are collected, consequently improving accuracy of section marking through the series. Jumbo diamond knives are more commonly commercially available (Diatome Ltd and Syntek) with the aim to provide a larger water surface area for section organisation and collection, together with various mechanisms of holding the section support substrate and/or water withdrawal. In addition, several researchers have developed alternative modifications, be it of either the diamond knife, boat or 'pick-up' strategies with the use of manipulators (Horstmann et al., 2012; Koike et al., 2017; Spomer et al., 2020; Wacker et al., 2016), or water withdrawal (Burel et al., 2018), development of a knife insert to control section order (Lee et al., 2020), or even the introduction of rotary magnets which (when combined with magnetic resin) result in the potential for collecting 1000's of sections onto a large silicon wafer (Templier, 2019)

Ultramicrotome modifications, with and without environmental chambers, have been commercialised, with the ARTOS-3D (Leica Microsystems) providing a programmed routine of serial sectioning parameters creating a set of ribbons for collection, or the ATUMtome (previously ATLUM, RMC) (Webster et al., 2015, Schifferer et al MCB: Volume Electron Microscopy Volume 179), or AutoCUTS systems (Li et al., 2017, Zhenjiang Lehua Technology Co.,Ltd), which are based on the concept of collecting 1000's of ordered, serial, sections on a continual reel of tape, which can then be transferred to wafers for imaging (Schalek et al., 2011). Thus, support substrate options range from coverslips, microscope slides, silicon wafers and tape, which can be treated (with charge or chemicals) or coated (with carbon, Indium titanium oxide) (Collman et al., 2015; Horstmann et al., 2012; Micheva & Smith, 2007). These treatments aid interactions between the substrate and water and sections during sectioning; the stability and flatness of sections on the support during storage and potential subsequent staining procedures; as well as flatness, conductivity and behaviour within the environment of the SEM during imaging. All of these factors need to be considered when planning a pure vEM experiment, however if correlative light and electron imaging of arrayed sections is required, then one needs to additionally consider properties of the substrate with respect to light microscopy imaging and light microscope configuration and specifications. With these workflows, it is useful to be aware that several microscope manufacturers either sell array tomography imaging software for light microscopes or alternative mechanisms for porting light microscopy data into the

SEM for easier correlation and re-location of ROI (Burel et al., 2018; Micheva & Smith, 2007).

Alternatively, light and electron microscopy can also be performed within the same system (Gabarre et al., 2021).

SEM hardware and software advances:

Comparatively, with respect to SBF-SEM and FIB-SEM, SEM imaging for array tomography is in principle simpler, as there is no need to co-ordinate function and timing with secondary equipment, (ultramicrotome or FIB) that is often manufactured by a third party. This also brings the benefits of not having to compromise optimal imaging parameters to fit with the need to avoid physical, beam-induced damage to the sample that would affect subsequent cutting/milling properties. Automated SEM-AT imaging requires a stable, high resolution electron beam; robust, reproducibly accurate, fine stage control; sensitive, high contrast detectors and reliable software. SEM manufacturers have been developing and improving the first three requirements for decades to the benefit of all SEM users, whilst the last requirement is an area where more recent developments have made the potential of array tomography accessible to the wider scientific communities.

Backscattered electron imaging of heavy metal contrasted biological material embedded in resin has been in use for the last twenty years, with the user performing a delicate juggling act, balancing the interactions between acceleration voltage, interaction volume, signal to noise, resolution, heavy metal incorporation into the sample, together with imaging speed or pixel dwell time. A recent advance that has been of particular benefit to array tomography imaging, has been the use of beam deceleration, or negative stage bias. Here, an electric field is generated over the stage/sample by a tuneable, differential voltage between the stage and the pole piece, which causes the primary electron beam to decelerate, but backscattered electrons from the sample to accelerate towards the detector (depending on exact SEM geometries). The result is more efficient electron collection and images which have a higher signal to noise ratio and/or can be more easily acquired at lower pixel dwell times, significantly increasing the speed of imaging. The concept itself is not novel, but the benefit it brings to backscattered electron imaging of resin sections has only recently been appreciated and exploited.

With the growing popularity of backscattered electron imaging, further development has gone into improving detector performance, specifically with low kV imaging in mind. Developments vary

from improving signal amplification, minimising interference, increasing diode size as well as new diode styles. These result in higher signal to noise images at low kV, with the reduced electron dose bringing the additional benefits of reduced charging artifacts. These newer generation sensitive detectors bring various points of added value, either enabling the imaging of challenging samples that have little contrast, the faster imaging of amenable samples, or a combination of the two.

Another area of development that is of particular use for array tomography, is the introduction of a large scan generator and image store, which allows large fields of view to be captured at high resolution e.g. 32k x 32k pixels, which at 5nm pixel size equates to a field of view of 160 μm x 160 μm (Carl Zeiss Microscopy GmbH., 2020; Eberle et al., 2015). From the point of view of a regular user, this means that for most (if not all) projects, montaging and subsequent stitching is not required for the final acquisition. This removes the need for imaging overlapping regions to allow alignment post acquisition, which brings benefits in time (both imaging and post-acquisition alignment and stitching) but also removes the risk of introducing artifacts to the sample, where parts of the sample that are imaged four times to generate the montage may be irreversibly marked.

If particularly larger ROI across many 1000's of sections are needed, dedicated instruments for high throughput array tomography are now commercially available. Zeiss's MultiSEM (Eberle et al., 2015) and Delmic's FAST-EM (Kruit & Zuidema, 2019; Zuidema & Kruit, 2020), whilst using different approaches, follow similar principles of splitting the primary electron beam and simultaneously rastering and collecting data from these 61 or 91 (Zeiss MultiSEM 505 or 506) or 64 (Delmic FAST-EM) parallel beams. These can generate high resolution data at an incredible rate (Delmic FAST-EM -100 megapixels/second, Zeiss MultiSEM 505/6 1.22 gigapixels/second), making these formidable technologies essential for large scale connectomics research.

With all these advances, it is important to note that a two or four fold improvement in any one aspect of this workflow can have an exponential impact on real world throughput. For example, use of stage bias, may decrease pixel dwell time from 5 μs to 2.5 μs , but with additional use of a sensitive detector could further reduce dwell time from 2.5 μs to 0.5 μs per pixel. When considered over a whole experiment, where billions of pixels are being acquired, this can result in an experiment taking hours rather than several days.

Prospects and future challenges:

Improvements in the areas of serial sectioning and collection are lowering the entry barrier for researchers wanting to take advantage of the potential of SEM-AT. In addition, with SEM-AT imaging being a software solution rather than requiring specialist hardware, SEM-AT is becoming an increasingly cost-effective, flexible and attractive prospect for those wishing to enter the field of vEM. Nevertheless, there remain challenges to be solved and improvements made, to enable everyday users to exploit the technique to its fullest potential.

Currently, it is relatively straightforward to collect hundreds of serial sections using the basic manual techniques we have described above. With the attention being given to this area, as demonstrated by the development of the automated techniques and of knife/knife boat modifications, it is likely that we will continue to see improvements, both commercial and “lab hacks”, to make it more user friendly and accessible to less experienced microtomists. Whilst obviously crucial, sectioning and collection is a relatively small part of the SEM-AT process in terms of time expenditure, thus the real gains to be made are in the field of imaging. Whilst still not quite at the level of TEM, the resolution and image quality of section imaging on a modern, appropriately equipped, SEM has proven easily sufficient for answering most cell biology research questions, e.g. imaging membranes, virus, membrane contacts, synaptic vesicles etc (Collman et al., 2015; Kataoka et al., 2019; Norris & Terasaki, 2021; Terasaki et al., 2013). Further improvements will undoubtedly be made, but as of this time the ultimate resolution of imaging is not the decisive factor when considering SEM-AT in most projects, rather it is the time taken to acquire the images that is the limiting step. Currently all systems require significant user input, early in the process. Whilst not technically demanding, further improvements in software automation, accuracy in section delineation, ROI placement, and feature tracking will surely reduce this input further. Faster more reliable autofocus and stigmation functions will improve both speed and quality of image acquisition, basic image processing “on the fly” during the acquisition process (e.g. stitching mosaics, or basic alignments) are also likely to aid image interpretation and save time post acquisition.

Even without further improvements, users can already quickly and relatively easily acquire several ultrastructural cell volumes per day, making statistical analysis of vEM data a realistic option and not a pipedream. This increase in throughput releases vEM access to a greater pool of researchers, bringing with it the computation demands of working with large data and the image

analysis challenges associated with the information dense vEM data, - for which many research laboratories and IT departments are ill prepared. These challenges are not unique to SEM-AT but common to all vEM approaches and whilst they are already known and being addressed by researchers, and communities (vEM, Neubias, COMULIS) worldwide, dissemination and implementation of these improvements will need to accelerate to keep pace with the efficiency of data acquisition.

As SEM-AT develops it is likely to become more commonplace both for routine 3D ultrastructural imaging, taking the burden of certain projects (for which it is better suited) from its vEM cousins, as well as filling a specialised niche. These may include samples with lots of bare resin, samples with a large number of ROI per section, as well as samples that were not amenable to other vEM techniques such as legacy samples with minimal metal contrasting en bloc. Continuing improvements and a critical mass of skilled operators will fully unlock the potential for biologists to leverage the unique power of SEM-AT as a vEM technique and drive forward research – across all disciplines.

Acknowledgements:

JJB and IJW are supported by core funding to the Laboratory for Molecular Cell Biology at University College London. The LMCB SEM-AT facility was set up with funding from the Wellcome Trust (218278/Z/19/Z) and UCL CEF contributions. The authors would like to thank Stephen Furzeland, Steve Murray, Anwen Bullen and Andy Yarwood, for helpful discussions.

References

Bang, B., & Bang, F. (1957). Graphic reconstruction of the third dimension from serial electron microphotographs. *Journal of Ultrastructure Research*, 1(2), 138–139.

Birch-Andersen, B. A. (1955). Reconstruction of the Nuclear Sites of *Salmonella typhimurium* from Electron Micrographs of Serial Sections. In *J. gen. Microbiol* (Vol. 13).

- Burel, A., Thérèse Lavault, M.-T., Clément Chevalier, C., Gnaegi, H., Prigent, S., Mucciolo, A., Dutertre, S. S., Humbel, B. M., Guillaudeux, T., & Kolotuev, I. (2018). *A targeted 3D EM and correlative microscopy method using SEM array tomography*.
<https://doi.org/10.1242/dev.160879>
- Cardona, A., Saalfeld, S., Schindelin, J., Arganda-Carreras, I., Preibisch, S., Longair, M., Tomancak, P., Hartenstein, V., & Douglas, R. J. (2012). TrakEM2 software for neural circuit reconstruction. *PLoS ONE*, 7(6).
<https://doi.org/10.1371/JOURNAL.PONE.0038011>
- Carl Zeiss Microscopy GmbH. (2020). *High Resolution and High Throughput Imaging of Tissue Samples Using The ATLAS™*. AZoNano.
<https://www.azonano.com/article.aspx?ArticleID=2724>
- Cattin, A. L., Burden, J. J., van Emmenis, L., MacKenzie, F. E., Hoving, J. J. A., Garcia Calavia, N., Guo, Y., McLaughlin, M., Rosenberg, L. H., Quereda, V., Jamecna, D., Napoli, I., Parrinello, S., Enver, T., Ruhrberg, C., & Lloyd, A. C. (2015). Macrophage-Induced Blood Vessels Guide Schwann Cell-Mediated Regeneration of Peripheral Nerves. *Cell*, 162(5), 1127–1139. <https://doi.org/10.1016/j.cell.2015.07.021>
- Chen, B., Yusuf, M., Hashimoto, T., Estandarte, A. K., Thompson, G., & Robinson, I. (2017). Three-dimensional positioning and structure of chromosomes in a human prophase nucleus. *Science Advances*, 3(7).
<https://doi.org/10.1126/SCIADV.1602231>
- Collman, F., Buchanan, J., Phend, K. D., Micheva, K. D., Weinberg, R. J., & Smith, S. J. (2015). Mapping Synapses by Conjugate Light-Electron Array Tomography. *Journal of Neuroscience*, 35(14), 5792–5807. <https://doi.org/10.1523/JNEUROSCI.4274-14.2015>

- de Schepper, S., Ge, J. Z., Crowley, G., Ferreira, L. S. S., Garceau, D., Toomey, C. E., Sokolova, D., Childs, T., Lashley, T., Burden, J. J., Jung, S., Sasner, M., Frigerio, C. S., & Hong, S. (2022). Perivascular SPP1 Mediates Microglial Engulfment of Synapses in Alzheimer's Disease Models. *BioRxiv*, 2022.04.04.486547.
<https://doi.org/10.1101/2022.04.04.486547>
- Deerinck, T. J., Bushong, E. A., Ellisman, M. H., & Thor, A. (2022). Preparation of Biological Tissues for Serial Block Face Scanning Electron Microscopy (SBEM). *Protocols.io*.
- Eberle, A. L., Selchow, O., Thaler, M., Zeidler, D., & Kirmse, R. (2015). Mission (im)possible - mapping the brain becomes a reality. *Microscopy (Oxford, England)*, 64(1), 45–55. <https://doi.org/10.1093/JMICRO/DFU104>
- Gabarre, S., Vernailen, F., Baatsen, P., Vints, K., Cawthorne, C., Boeynaems, S., Michiels, E., Vandael, D., Gounko, N. v., & Munck, S. (2021). A workflow for streamlined acquisition and correlation of serial regions of interest in array tomography. *BMC Biology*, 19(1), 1–15. <https://doi.org/10.1186/S12915-021-01072-7/FIGURES/6>
- Harris, K. M., Perry, E., Bourne, J., Feinberg, M., Ostroff, L., & Hurlburt, J. (2006). Uniform Serial Sectioning for Transmission Electron Microscopy. *The Journal of Neuroscience*, 26(47), 12101–12103. <https://doi.org/10.1523/JNEUROSCI.3994-06.2006>
- Horstmann, H., Körber, C., Sätzler, K., Aydin, D., & Kuner, T. (2012). Serial section scanning electron microscopy (S 3EM) on silicon wafers for ultra-structural volume imaging of cells and tissues. *PLoS ONE*, 7(4).
<https://doi.org/10.1371/journal.pone.0035172>
- Kataoka, M., Ishida, K., Ogasawara, K., Nozaki, T., Satoh, Y.-I., Sata, T., Sato, Y., Hasegawa, H., & Nakajima, N. (2019). Serial Section Array Scanning Electron Microscopy

Analysis of Cells from Lung Autopsy Specimens following Fatal A/H1N1 2009
Pandemic Influenza Virus Infection. *Journal of Virology*, 93(19).

<https://doi.org/10.1128/JVI.00644-19>

Koike, T., Kataoka, Y., Maeda, M., Hasebe, Y., Yamaguchi, Y., Suga, M., Saito, A., & Yamada, H. (2017). A Device for Ribbon Collection for Array Tomography with Scanning Electron Microscopy. *Acta Histochem. Cytochem*, 50(5), 135–140.

<https://doi.org/10.1267/ahc.17013>

Kruit, P., & Zuidema, W. (2019). A Dedicated Multi-Beam SEM for Transmission Imaging of Thin Samples. *Microscopy and Microanalysis*, 25(S2), 1034–1035.

<https://doi.org/10.1017/S1431927619005907>

Lee, T. J., Yip, M. C., Kumar, A., Lweallen, C. F., Bumbarger, D. J., Reid, R. C., & Forest, C. R. (2020). Capillary-and Stokes-based trapping of serial sections for scalable 3D-EM connectomics. *ENeuro*, 7(2). <https://doi.org/10.1523/ENEURO.0328-19.2019>

Li, X., Ji, G., Chen, X., Ding, W., Sun, L., Xu, W., Han, H., & Sun, F. (2017). Large scale three-dimensional reconstruction of an entire *Caenorhabditis elegans* larva using AutoCUTS-SEM. *Journal of Structural Biology*, 200(2), 87–96.

<https://doi.org/10.1016/J.JSB.2017.09.010>

Lowe, D. G. (2004). Distinctive Image Features from Scale-Invariant Keypoints. In *International Journal of Computer Vision* (Vol. 60, Issue 2).

Micheva, K. D., & Smith, S. J. (2007). Array Tomography: A New Tool for Imaging the Molecular Architecture and Ultrastructure of Neural Circuits. *Neuron*, 55(1), 25–36.

<https://doi.org/10.1016/J.NEURON.2007.06.014>

Norris, R. P., & Terasaki, M. (2021). Gap junction internalization and processing in vivo: A 3D immuno-electron microscopy study. *Journal of Cell Science*, 134(1).

<https://doi.org/10.1242/JCS.252726/VIDEO-3>

- Peddie, C. J., Genoud, C., Kreshuk, A., Meechan, K., Micheva, K. D., Narayan, K., Pape, C., Parton, R. G., Schieber, N. L., Schwab, Y., Titze, B., Verkade, P., Weigel, A., & Collinson, L. M. (2022). Volume electron microscopy. *Nature Reviews Methods Primers*, 2(1), 51. <https://doi.org/10.1038/s43586-022-00131-9>
- Schalek, R., Kasthuri, N., Hayworth, K., Berger, D., Tapia, J. C., Morgan, J. L., Turaga, S. C., Fagerholm, E., Seung, H. S., & Lichtman, J. W. (2011). Development of High-Throughput, High-Resolution 3D Reconstruction of Large-Volume Biological Tissue Using Automated Tape Collection Ultramicrotomy and Scanning Electron Microscopy. *Microscopy and Microanalysis*, 17(2), 966. <https://doi.org/10.1017/S1431927611005708>
- Schindelin, J., Arganda-Carreras, I., Frise, E., Kaynig, V., Longair, M., Pietzsch, T., Preibisch, S., Rueden, C., Saalfeld, S., Schmid, B., Tinevez, J. Y., White, D. J., Hartenstein, V., Eliceiri, K., Tomancak, P., & Cardona, A. (2012). Fiji: An open-source platform for biological-image analysis. *Nature Methods*, 9(7), 676–682. <https://doi.org/10.1038/NMETH.2019>
- Spomer, W., Hofmann, A., Veith, L., & Gengenbach, U. (2020). Chapter 5 A Low-Tech Approach to Serial Section Arrays. *Volume Microscopy: Multiscale Imaging with Photons, Electrons, and Ions, Neuromethods*, 155. https://doi.org/10.1007/978-1-0716-0691-9_5
- Stalling, D., Westerhoff, M., & Hege, H.-C. (2005). *amira: A Highly Interactive System for Visual Data Analysis* / Elsevier Enhanced Reader. Visualization Handbook. <https://reader.elsevier.com/reader/sd/pii/B978012387582250040X?token=50F085B09A2C7DB34FE095B2C0DC8268EAA77ACE74F2C591E48FA3D633B28D2A837404E4F8F60D2508EA79ADC2D903AE&originRegion=eu-west-1&originCreation=20211005103536>

- Started, G., Images, A., Alignment, M. I., Alignment, A. I., Information, G. Q., & Topics, S. H. (2013). IMOD User ' s Guide for Version 3 . 9. *Image (Rochester, N.Y.)*, 1–17.
- Templier, T. (2019). MagC, magnetic collection of ultrathin sections for volumetric correlative light and electron microscopy. *ELife*, 8. <https://doi.org/10.7554/eLife.45696>
- Terasaki, M., Shemesh, T., Kasthuri, N., Klemm, R. W., Schalek, R., Hayworth, K. J., Hand, A. R., Yankova, M., Huber, G., Lichtman, J. W., Rapoport, T. A., & Kozlov, M. M. (2013). XStacked endoplasmic reticulum sheets are connected by helicoidal membrane motifs. *Cell*, 154(2), 285. <https://doi.org/10.1016/j.cell.2013.06.031>
- Wacker, I., Spomer, W., Hofmann, A., Thaler, M., Hillmer, S., Gengenbach, U., & Schröder, R. R. (2016). Hierarchical imaging: A new concept for targeted imaging of large volumes from cells to tissues. *BMC Cell Biology*, 17(1). <https://doi.org/10.1186/s12860-016-0122-8>
- Wanner, A. A., Kirschmann, M. A., & Genoud, C. (2015). Challenges of microtome-based serial block-face scanning electron microscopy in neuroscience. *Journal of Microscopy*, 259(2), 137. <https://doi.org/10.1111/JMI.12244>
- Webster, P., Bentley, D., & Kearney, J. (2015). The ATUMtome for automated serial sectioning and 3-dimaging. *Microscopy and Analysis*, 29(2), 19–23.
- White, J. G., Southgate, E., Thomson, J. N., & Brenner, S. (1986). The structure of the nervous system of the nematode *Caenorhabditis elegans* . *Philosophical Transactions of the Royal Society of London. B, Biological Sciences*, 314(1165), 1–340. <https://doi.org/10.1098/RSTB.1986.0056>
- Xu, C. S., Hayworth, K. J., Lu, Z., Grob, P., Hassan, A. M., García-Cerdán, J. G., Niyogi, K. K., Nogales, E., Weinberg, R. J., & Hess, H. F. (2017). Enhanced FIB-SEM systems for large-volume 3D imaging. *ELife*, 6. <https://doi.org/10.7554/ELIFE.25916>

Zuidema, W., & Kruit, P. (2020). Transmission imaging on a scintillator in a scanning electron microscope. *Ultramicroscopy*, 218, 113055.

<https://doi.org/10.1016/J.ULTRAMIC.2020.113055>

Figure Legends:

Figure 1: Summary of the described SEM-AT workflow.

A) Preserved, heavy metal contrasted sample is embedded in a resin block and mounted for trimming. B) Asymmetric ultrathin sections, with parallel leading and trailing edges, form a neat ribbon during sectioning. C) Multiple ribbons split into suitable lengths are collected in sequence order on an ITO coated coverslip to form an array of many hundred sections. D) Coverslip is mounted onto an SEM stub via carbon sticky tab with silver DAG to improve conductivity. E) The array in its entirety is mapped into the software at low resolution/high speed. F) Section outlines are marked semi-automatically, a circular ROI applied to one section is automatically propagated to all sections marked. G) ROI acquired at the required resolution across selected sections. H) Post acquisition, data is aligned and, XZ and YZ projections are used to assess the alignment.

Figure 2: Comparison of the ssTEM and SEM-AT workflows.

A) Resin embedded sample

For ssTEM a) A small blockface is trimmed from the sample leading to b) small area sections. c) Short <2mm ribbons are docked next to each other to a maximum <1mm width. d) Each ribbon collection described in c) is collected onto separate delicate 2mmx1mm formvar coated slot grids.

For SEM-AT i) A larger blockface can be trimmed leading to ii) larger area sections. iii) Longer <20mm ribbons are docked next to each other to a width <20mm. iv) The whole array of hundreds of sections is collected in a single action onto one robust, rigid substrate.

Figure 3: Simple modifications to the knife and microtome for inexpensive and easy collection of arrays of hundreds of sections on coverslips.

A) A metal paperclip is “unfolded”, trimmed to appropriate length depending on knife width and moulded to shape using pliers. B) End view shows the paperclip folded over the edges of the knife boat on both sides and running across the bottom of the trough. The side view shows the paperclip positioned such that when the collection substrate is inserted into the knife boat, the lower edge rests stably against the paperclip at the bottom of the trough, and the upper edge protrudes from the water by 1-2mm and rests against the rear edge of the knife boat. C) A photo of the apparatus shows the coverslip protruding from the water on the left, the paperclip appropriately placed and secured with tape to support it, and the water withdrawal needle and tubing in position on the far side. D) Illustrates the region of the coverslip coated with poly-L-lysine. E) A pen mark on the edge of the knife boat marks 18mm perpendicular to the knife edge, to judge appropriate points to break ribbons. F) The water withdrawal needle is attached to silicon tube, which is loosely taped to the microtome to avoid transfer of vibrations and terminates in a syringe for manual water withdrawal.

Figure 4: Geometry of blockface preparation: impact upon serial section sizes

(A) A block prepared for sectioning shown from the side. Simple trigonometry reveals that given side slope angles of 20° , then over 600, 70nm sections the sections from this blockface will increase in size by over $30\mu\text{m}$ in both X and Y dimensions. (B) A top view of the trimmed blockface. Given that the individual edges may vary in what angle they have been trimmed to (10° - 30°), the resulting later sections may have changed not just in overall size, but also relative geometry, making section outline templates as section markers, challenging to place accurately.

Figure 5: Section and ROI defining methods

(A) Schematic of a section containing a feature of interest. (B) The traditional method of section marking via outlining the section. (C) An alternative method where a rectangle is placed, rotated to be parallel with the section leading edge and centred on a feature, constant throughout the section range. (D) An oval ROI large enough to cover the feature of interest but without wasting time imaging rectangle corners with no relevant information. (E) A rectangle ROI scaled generously to account for section and ROI placement inaccuracies and still image all of the feature of interest. (F) A ROI marker scaled tight to the feature of interest in section 1, but that due to section and ROI placement inaccuracies misses important parts of the feature of interest in imaging subsequent sections.

Video Captions:

Video 1: Contact cement application

Video 2: Section splitting

Video 3: Water withdrawal and section collection

Video 4: Ribbon scans

Video 5: Automated section marking

Figures:

Figure 1: Summary of the described SEM-AT workflow.

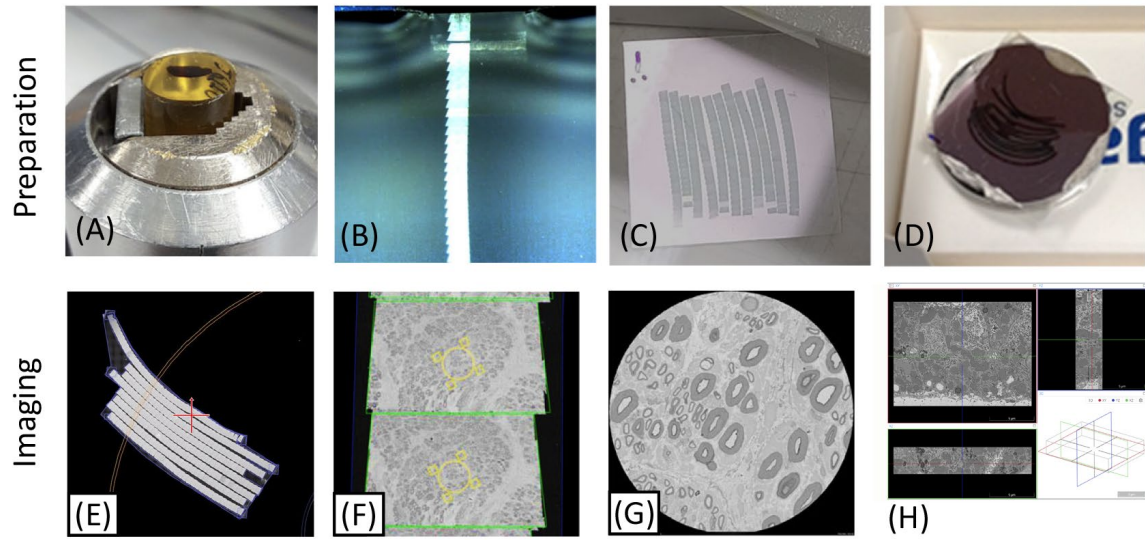


Figure 2: Comparison of the ssTEM and SEM-AT workflows.

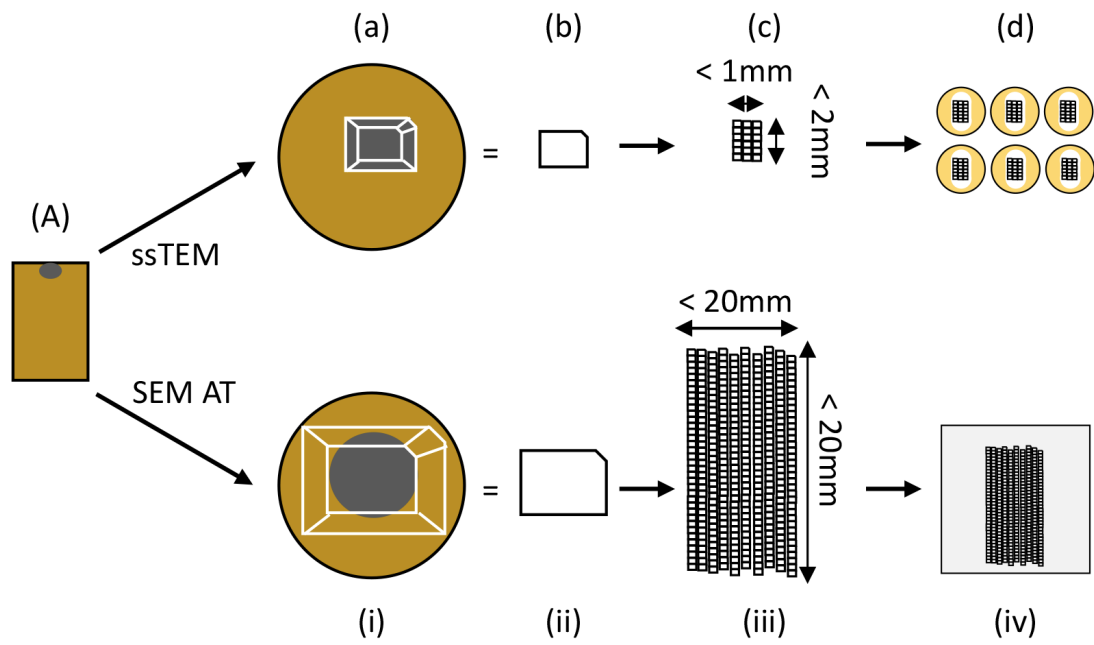


Figure 3: Simple modifications to the knife and microtome for inexpensive and easy collection of arrays of hundreds of sections on coverslips.

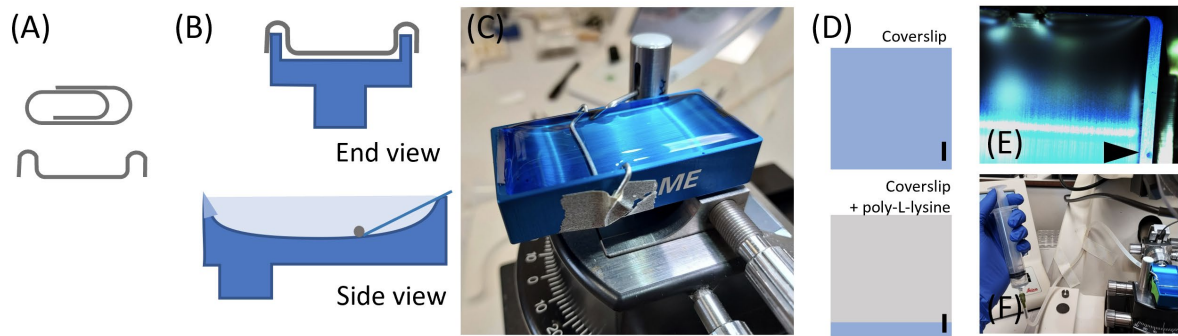


Figure 4: Geometry of blockface preparation: impact upon serial section sizes

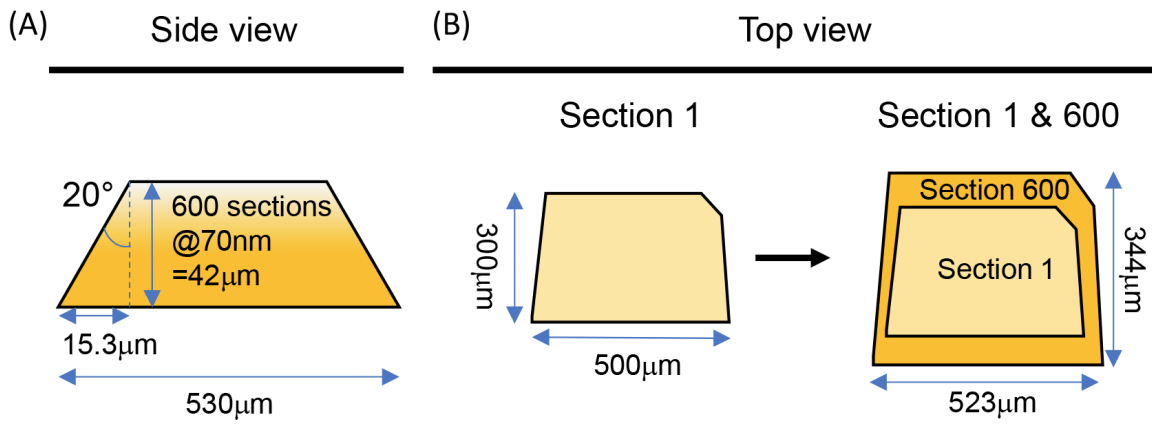


Figure 5: Section and ROI defining methods

